

# Hanbury Brown and Twiss Interferometry with respect to 2<sup>nd</sup> and 3<sup>rd</sup>-order event planes in Au+Au collisions at $\sqrt{s_{NN}} = 200$ GeV

**Takafumi Niida for the PHENIX Collaboration**

University of Tsukuba, 1-1-1 Tennoudai, Tsukuba, Ibaraki 305-8571, Japan

E-mail: niida@bnl.gov

**Abstract.** Azimuthal angle dependence of HBT interferometry have been measured with respect to 2<sup>nd</sup> and 3<sup>rd</sup>-order event planes in Au+Au collisions at  $\sqrt{s_{NN}} = 200$  GeV at the PHENIX experiment. The 3<sup>rd</sup>-order dependence of a Gaussian source radii was clearly observed as well as 2<sup>nd</sup>-order dependence. The result for 2<sup>nd</sup>-order indicates that the initial source eccentricity is diluted but still retain the initial shape at freeze-out, while the result for 3<sup>rd</sup>-order implies that the initial triangularity vanishes during the medium evolution, which is supported by a Gaussian source model and Monte-Carlo simulation.

## 1. Introduction

Initial density distribution in a heavy ion collision fluctuates due to finite number of participating nucleons [1], which leads to higher harmonic flow as recently measured at RHIC and the LHC [2, 3, 4]. Such spatial fluctuations may be preserved until kinetic freeze-out, depending on the strength of the initial fluctuations, the flow profile, the expansion time, and viscosity of the created matter. Detailed study of the spatial distribution at the freeze-out is needed to reveal these properties with the picture of the space-time evolution.

Hanbury Brown and Twiss (HBT) interferometry [5] is a powerful tool to study the space-time extent of a particle emitting source in the heavy ion collision. Azimuthal angle dependence of Gaussian source radii via two-pion interferometry have been recently measured with respect to 2<sup>nd</sup> and 3<sup>rd</sup>-order event planes with PHENIX in Au+Au collisions at  $\sqrt{s_{NN}} = 200$  GeV [11]. We present these results and discuss triangularity of the source as well as the eccentricity at freeze-out by comparing with recent hydrodynamic models.

## 2. Analysis

Analysis was performed using data collected by the PHENIX experiment in 2007 running period, where the number of events were about 4.2 billion events. The event planes were determined by the Reaction Plane Detector (RXNP) [9] by measuring azimuthal anisotropy of emitted particles. The azimuthal distribution of emitted particles is defined in a form of Fourier expansion:

$$\frac{dN}{d\phi} \propto 1 + 2 \sum_n v_n \cos[n(\phi - \Psi_n)], \quad (1)$$



where  $\phi$  is azimuthal angle of emitted particles,  $v_n$  is  $n^{\text{th}}$ -order Fourier coefficient representing the strength of anisotropic flow, and  $\Psi_n$  is azimuthal angle of  $n^{\text{th}}$ -order event plane. The resolution of the event plane is defined as  $\text{Res}\{\Psi_n\} = \langle \cos[n(\Psi_n^{\text{obs}} - \Psi_n^{\text{true}})] \rangle$ , and 75% for 2<sup>nd</sup>-order and 32% for 3<sup>rd</sup>-order at maximum, which were estimated using the event plane correlation between forward and backward RXNPs. Particle identification was performed by combining time-of-flight from the collision vertex to the electromagnetic calorimeter with reconstructed momentum and flight path length in the magnetic field, where  $\pi/K$  separation was achieved up to  $\sim 1$  GeV/ $c$ .

The experimental correlation function is defined as  $C_2 = A(q)/B(q)$ , where  $A(q)$  is the relative momentum ( $q$ ) distribution of pair particles in the same event and  $B(q)$  is that in different events but with similar centrality, vertex position, and the event plane. The pair analysis was performed with the Bertsch-Pratt parameterization [6, 7] and the fitting function is based on core-halo model [8] taking into account the Coulomb interaction and the long-lived resonance decays:

$$C_2 = C_2^{\text{core}} + C_2^{\text{halo}} = [\lambda(1 + G)F_c] + [1 - \lambda], \quad (2)$$

$$G = \exp(-R_s^2 q_s^2 - R_o^2 q_o^2 - R_l^2 q_l^2 - 2R_{os}^2 q_o q_s), \quad (3)$$

where  $F_c$  is the Coulomb correction factor and  $\lambda$  determines the fraction of pairs in the core. The  $R_\mu$  ( $\mu = s, o, l$ ) represents Gaussian source radii called HBT radii and  $R_{os}$  is the cross term between  $q_o$  and  $q_s$  directions. It is known that the finite resolution of the event plane smears azimuthal angle dependence of HBT radii. Therefore a model independent correction [10] was applied in this analysis.

### 3. Results

Figure 1 shows the extracted HBT radii of charged pions as a function of azimuthal pair angle  $\phi$  relative to 2<sup>nd</sup> and 3<sup>rd</sup>-order event planes in  $0.2 < k_T < 2.0$  GeV/ $c$  for two centrality bins, where upper panels ((a)-(d)) for 2<sup>nd</sup>-order and bottom panels ((e)-(h)) for 3<sup>rd</sup>-order. In 2<sup>nd</sup>-order dependence, the oscillation of  $R_s^2$ ,  $R_o^2$ , and  $R_{os}^2$  are clearly seen, and they seem to become larger in 20-30% than in 0-10%, where  $R_o^2$  shows the opposite sign of the oscillation to  $R_s^2$ . This trend could be understood by out-of-plane extended elliptical source as seen in the STAR experiment [12]. In 3<sup>rd</sup>-order dependence, the finite but relatively weaker oscillations are observed, where  $R_s^2$  and  $R_o^2$  have the same sign of the oscillation unlike the 2<sup>nd</sup>-order case.

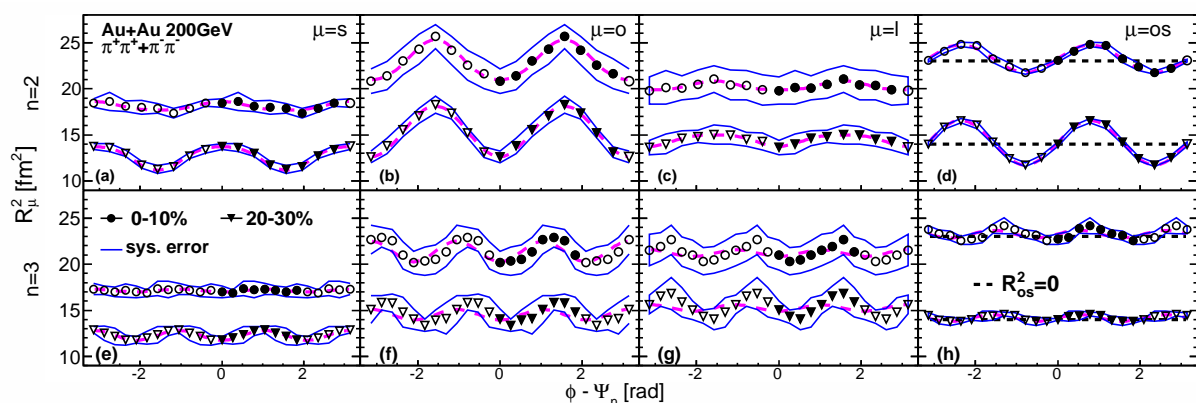


**Figure 1.** HBT radii of charged pions with respect to 2<sup>nd</sup> and 3<sup>rd</sup>-order event planes in  $0.2 < k_T < 2.0$  GeV/ $c$  and two centrality bins. The filled symbols show the extracted HBT radii and the open symbols are reflected by symmetry around  $\phi - \Psi_n = 0$ . Bands of two thin lines represent the systematic uncertainties and magenta dashed lines are fit functions by Eq. (4).

In order to extract the oscillation amplitudes, the azimuthal angle dependence of HBT radii was fitted by the following formula [13]:

$$\begin{aligned} R_\mu^2(\phi - \Psi_m) &= R_{\mu,0}^2 + 2 \sum_{n=m,2m} R_{\mu,n}^2 \cos[n(\phi - \Psi_m)] \quad (\mu = s, o, l), \\ R_\mu^2(\phi - \Psi_m) &= 2 \sum_{n=m,2m} R_{\mu,n}^2 \sin[n(\phi - \Psi_m)] \quad (\mu = os), \end{aligned} \quad (4)$$

where  $R_{\mu,n}^2$  are the Fourier coefficients. The extracted 2<sup>nd</sup>-order Fourier coefficients relative to 0<sup>th</sup> ones are plotted as a function of initial source anisotropy  $\varepsilon_n$  calculated by Monte-Carlo Glauber simulation in Fig. 2. Final source eccentricity given by  $2R_{s,2}^2/R_{s,0}^2$  [13] shows a half of  $\varepsilon_n$ , which indicates that the source eccentricity is reduced during the system evolution but still retain initial shape extended out-of-plane direction. For 3<sup>rd</sup>-order, there is no significant centrality ( $\varepsilon_n$ ) dependence, but  $R_{s,3}^2/R_{s,0}^2$  is almost equal to zero or slightly negative (positive) in all centralities.

Figure 3 shows  $k_T$  dependence of 3<sup>rd</sup>-order oscillation amplitudes in two centrality bins. The  $R_{s,3}^2/R_{s,0}^2$  doesn't show any clear dependency on  $k_T$  unlike 2<sup>nd</sup>-order [14], while the magnitudes of  $R_{o,3}^2/R_{o,0}^2$  increase with  $k_T$  in both centralities. Calculations from the Gaussian source model including 3<sup>rd</sup>-order triangular flow and spatial deformation [15] are compared, where two extreme cases, finite triangular flow without spatial deformation ( $\bar{\varepsilon}_3 = 0, \bar{v}_3 = 0.25$ ) and non-triangular flow with spatial triangular deformation ( $\bar{\varepsilon}_3 = 0.25, \bar{v}_3 = 0$ ), are shown. The  $R_{o,3}^2$  favors the deformed flow case, while  $R_{s,3}$  matches only at low  $k_T$  region. Result from Monte-Carlo simulation [11] with finite triangular flow and non-spatial deformation is also compared as broken lines, which is qualitatively consistent with the Gaussian source model. We note that both calculations have a discrepancy of  $R_{s,3}^2$  at higher  $k_T$ , but it may be solved by a full hydrodynamic calculation [16].

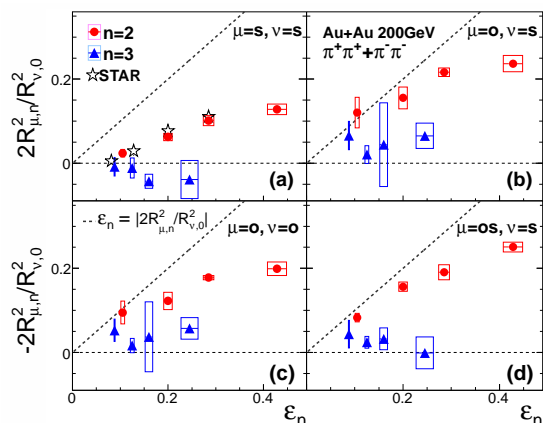


**Figure 2.** Oscillation amplitudes relative to their averages for 2<sup>nd</sup> and 3<sup>rd</sup>-order event plane dependences as a function of initial spatial anisotropy.

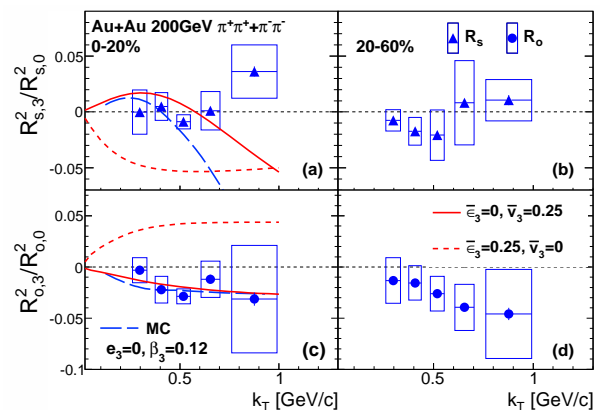


**Figure 3.**  $k_T$  dependence of 3<sup>rd</sup>-order oscillation amplitudes relative to their averages for  $R_s^2$  and  $R_o^2$ , where the Gaussian source model (solid and dashed lines) [15] and a Monte-Carlo simulation (broken line) [11] are compared.

Hydrodynamic models suggests that the higher-order spatial anisotropies have different responses to the time evolution of the system [17, 18]. Especially the sign of 3<sup>rd</sup>-order anisotropy ( $\varepsilon_3$ ) turns over faster than 2<sup>nd</sup>-order ( $\varepsilon_2$ ) during the system evolution. Therefore the detailed comparison with the event-by-event hydrodynamics would provide us further description of the system evolution, and information on the initial conditions and the properties of the medium.

#### 4. Summary

We have presented results on HBT measurements with respect to 2<sup>nd</sup> and 3<sup>rd</sup>-order event planes in Au+Au collisions at  $\sqrt{s_{NN}} = 200$  GeV at the PHENIX experiment. The observed oscillations of HBT radii for 2<sup>nd</sup>-order event plane indicate the elliptical source shape at the end of the system evolution, while finite oscillation of  $R_o$  for 3<sup>rd</sup>-order event plane would be mainly driven by triangular flow at final state and very weak oscillation of  $R_s$  implies that the spatial triangular deformation almost vanishes during the system evolution.

#### References

- [1] B. Alver and G. Roland, *Phys. Rev. C* **81**, 054905 (2010)
- [2] A. Adare *et al.* (PHENIX Collaboration), *Phys. Rev. Lett.* **107**, 252301 (2011)
- [3] K. Aamodt *et al.* (ALICE Collaboration), *Phys. Rev. Lett.* **107**, 032301 (2011)
- [4] G. Aad *et al.* (ATLAS Collaboration), *Phys. Rev. C* **86**, 014907 (2012)
- [5] R. Habury Brown and R. Q. Twiss, *Nature* **178**, 1046 (1956)
- [6] S. Pratt, *Phys. Rev. D* **33**, 72 (1986)
- [7] G. Bertsch, M. Gong, and M. Tohyama, *Phys. Rev. C* **37**, 1896 (1988)
- [8] Y. Sinyukov, R. Lednicky, S. V. Akkelin, J. Pluta, and B. Erasmus, *Phys. Lett. B* **432**, 248 (1998)
- [9] E. Richardson *et al.* (PHENIX Collaboration), *Nucl. Instrum. Methods Phys. Res., Sect. A* **636**, 99 (2011).
- [10] U. Heinz, A. Hummel, M. A. Lisa and U. A. Wiedemann, *Phys. Rev. C* **66**, 044903 (2002)
- [11] A. Adare *et al.* (PHENIX Collaboration), *Phys. Rev. Lett.* **112**, 222301 (2014)
- [12] J. Adams *et al.* (STAR Collaboration), *Phys. Rev. Lett.* **93**, 012301 (2004)
- [13] F. Retière and M. A. Lisa, *Phys. Rev. C* **70**, 044907 (2004)
- [14] T. Niida for the PHENIX Collaboration, *J. Phys.: Conf. Ser.* **422**, 012005 (2013)
- [15] C. J. Plumberg, C. Shen and U. Heinz, *Phys. Rev. C* **88**, 044914 (2013)
- [16] C. J. Plumberg, talk given at Workshop on Particle Correlations and Femtoscopy, Acireale, Nov. 5-8, 2013
- [17] D. Teaney and L. Yan, *Phys. Rev. C* **83**, 064904 (2011)
- [18] C. Nonaka, talk given at Workshop on Initial Fluctuations and Final Correlations, Chengdu, Aug. 11-14, 2013